

# Reducing Activation-related Bias in FMRI Registration

Luis Freire<sup>12</sup>, Jeff Orchard<sup>3</sup>, Mark Jenkinson<sup>1</sup>, and Jean-François Mangin<sup>4</sup>

<sup>1</sup> Functional MRI Centre of the Brain, Oxford University, OX3 9DU, Oxford, U.K.

<sup>2</sup> Instituto de Biofísica e Engenharia Biomédica, FCUL, 1749-016 Lisboa, Portugal.

<sup>3</sup> School of Computer Science, University of Waterloo, Waterloo N2L 3G1, Canada.

<sup>4</sup> Service Hospitalier Frédéric Joliot, CEA, 91401 Orsay, France.

**Abstract.** The presence of cerebral activation may bias motion correction estimates when registering FMRI time series. This problem may be solved through the use of specific registration methods, which incorporate or down-weight cerebral activation confounding signals during registration. In this paper, we evaluate the performance of different registration methods specifically designed to deal with the problem of activation presence. The methods studied here yielded better results than the traditional approaches based on least square metrics, almost totally eliminating the activation-related confounds.

## 1 Introduction

The problem of subject motion is of particular importance in FMRI studies, due to the small amplitude of the signal changes induced by cerebral activation. Indeed, signal variations introduced by slight movements can easily hide the BOLD signal features related to cognitive tasks, or lead to the appearance of false activations. Due to the lack of perfect and comfortable immobilization schemes, neuroimaging researchers often prefer to rely on retrospective motion correction of the FMRI time series. However, optimal registration of the time-series is not sufficient to correct for all signal changes due to subject motion during data acquisition.

In practice, an important confounding effect may still be introduced during the estimation of motion parameters. This confounding effect relates to the fact that the presence of activation may systematically bias the motion estimates, rendering them correlated with the activation profile (even in the absence of subject motion) [1]. This effect is particularly significant when motion estimates are obtained using similarity measures based on least squares metrics. The consequence may be the appearance of spurious activations along brain edges after statistical analysis. Moreover, this systematic bias is likely to render invalid any attempt to correct other motion-related artifacts by using motion parameters as regressors of no-interest.

A standard approach to reduce the activation-related bias in motion estimates consists of using a robust estimator [2, 3], for instance a Geman-McClure

M-estimator. In [4], the suitability of this estimator was assessed in the context of FMRI registration. This estimator, however, was not sufficient to completely discard activation-related correlations in the estimation of motion parameters. More recently, two new methods dedicated to FMRI registration were proposed in [5, 6].

In this paper, we evaluate the robustness of these two least-squares-based registration methods in the presence of activation. The fact that the proposed methods rely on two different computational frameworks, which differ in the interpolation and optimization schemes, has motivated the inclusion of the results obtained by conventional least-squares-based methods implemented under each computational framework. The robustness of the different methods is first evaluated using two artificial time series, produced in order to simulate a situation with absence of subject motion, and another with true activation-correlated motion. The different methods are finally tested on three actual time series obtained from human subjects in a 3T magnet.

## 2 Materials

### 2.1 Similarity Measures

In this paper, we have compared four registration methods, which are outlined next:

1. **Least Squares (LS1 and LS2)**. The least squares similarity measure is calculated through the sum of the squared residual difference between voxel pairs, for a given rigid-body transformation,  $T$ . For two images  $A$  and  $B$ , yielding the intensity pair of values  $(a, b)$  for voxel  $i$ , the least squares cost function is defined as

$$LS(A, B; T) = \sum_i (A_i - B_i^T)^2, \quad (1)$$

in which  $B_i^T$  is the resampled value of image  $B$  at voxel  $i$  after the geometric transformation  $T$  has been applied. The LS registration methods are based on two distinct computational frameworks. The first uses cubic-spline interpolation [7] under a Powell optimization scheme [8]. This LS implementation will be referred to as LS1. The second method relies on the computation of exact intensity derivatives introduced by a simple fixed-point iteration method. This second LS implementation will be referred to as LS2.

To prevent each method from being trapped in local minima, spatial smoothing is applied in both methods by convolving the image with a 3D Gaussian kernel with FWHM value set to 8 mm.

2. **Dedicated Least Squares (DLS)**. This is the registration method that imposes the strictest down-weighting of voxels that potentially bias motion estimates. It relies on a dedicated approach, which runs on a two-stage registration. After the first stage, which is identical to LS1, a rough mask intended

to include all activated areas, is obtained. During the second motion estimation, the voxels inside a dilated version of the activation mask are discarded from the calculation of the similarity measure. It should be noted that this mask may include some spurious activations stemming from a biased initial motion correction, which shall not be a problem if spurious activations are not too wide. An illustration of a discarding mask is provided in Figure 1 (*left*).

3. **Simultaneous Registration and Activation Detection (SRA).** The fourth method is the SRA, which attempts to overcome the problem of activation bias by incorporating the effects of the activation into the registration problem.

Least-squares registration involves finding the motion parameters  $x$  that minimize the sum of squared differences between the volumes  $A$  and  $B$ . Using a linear approximation to the motion transformation, this means solving

$$A = B + Gx, \quad (2)$$

in the least-squares sense, where the matrix  $G$  is the derivative of the transformation with respect to the motion parameters. In this case, consider the volumes  $A$  and  $B$  to be column vectors. Similarly, the formulation of activation detection using the general linear model,

$$A = B + yH, \quad (3)$$

lends itself to solving for the coefficients of activation,  $y$ , in a least-squares sense. Here,  $A$  and  $B$  can be thought of as voxel time series stored as row-vectors, while  $H$  holds the stimulus regressors in its rows. Since the volumes are stored in columns, and voxel time series are stored in rows, an entire dataset can be stored in a single matrix. Using this notation, an FMRI dataset can be modeled as a baseline dataset ( $B$ ), plus a motion component ( $Gx$ ), plus an activation component ( $yH$ ). Hence, we have the model:

$$A = B + Gx + yH. \quad (4)$$

A least-squares solution  $(X, Y)$  can easily be found using matrix factoring techniques or by an iterative method. However, it can be shown that the solution is not unique. Adding a regularization constraint that favours sparse activation maps has been shown to work on simulated FMRI datasets [6].

### 3 Description of the Experiments

#### 3.1 FMRI acquisitions

We have used a set of three FMRI studies, corresponding to three different subjects. The images were acquired on a Bruker scanner operating at 3T. Volume geometry is  $(64 \times 80 \times 18, 3.75 \text{ mm} \times 3.75 \text{ mm} \times 6.00 \text{ mm})$ . A block design was used to assess visual activation, in which two tasks were repeatedly presented to subjects following a box-car design. Each task had a duration of 18 s (corresponding to 9 volumes), and was repeated 10 times, yielding 180 images.

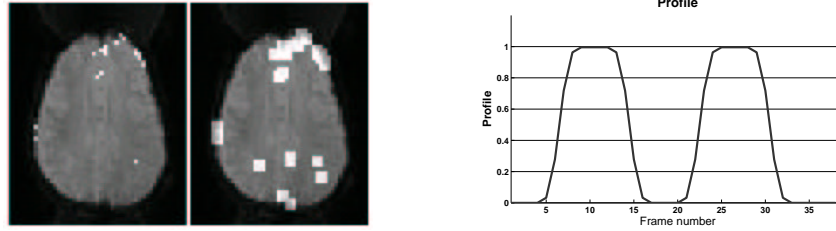


**Fig. 1.** (*Left*): example of the DLS discard mask with the estimated activated regions and activation mask obtained by dilation of activated regions. (*Right*): activation profile used to generate the simulated time series.

### 3.2 Experiments with Simulated Time Series

**Motionless Simulated Time Series:** The evaluation of the different registration methods is first performed using an artificial time series designed to simulate an activation process in the absence of subject motion. This was done by duplicating a reference image forty times and adding an activation-like signal change to some voxels in order to mimic a cognitive activation process. The activation time profile is shown in Figure 1 (*right*).

The added activation pattern was obtained using SPM99, after resampling the first actual time series with LS1 motion estimates (the activation pattern has a size of 6.7% of the brain and the mean activation level was set to 2% of brain mean value). To simulate the effects of thermal noise, Rician noise was added to the dataset by applying Gaussian noise (standard deviation of 2% of the mean brain value) to both the real and imaginary components. The four registration methods are then applied. For each registration method, we also compute the Pearson’s correlation coefficient of the 6 estimated motion parameters with the cognitive task profile. For the DLS method, the activation mask was obtained by statistical inference of the resampled simulated time series, according to [5].

The results for the simulated time series are presented in Figure 2. One can see that the DLS and the SRA registration methods can effectively reduce the bias in motion estimates introduced by the presence of activation. Substantial reductions in the correlation coefficients can also be observed in Table 1 (*left*).

**Simulated Time Series with True Correlated Motion:** The elaboration of this simulated time series is similar to the previous one, except that true activation-correlated motion was added. This is not an uncommon situation in real studies (for instance, if the subject is asked to speak) and, in fact, the consequences of a poor alignment may be disastrous in this situation. The simulated true correlated motion, which comprises translations in  $x$  and  $y$  directions, follows the same profile as the activation, with maximum amplitude in both directions of 2 mm. In order to minimize interpolation-related artifacts, Fourier interpolation in  $k$ -space was used, which is in accordance with the 2-D ( $x - y$  plane) signal acquisition process.

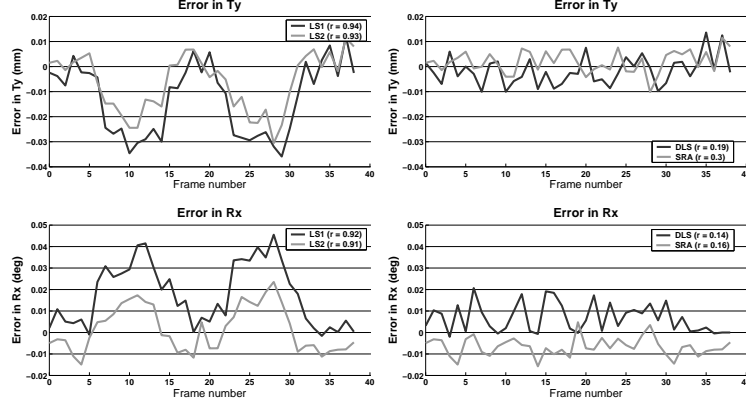


**Fig. 2.** Registration errors for the parameters  $t_y$  and  $r_x$  for the motion-free simulated time series. Graphs refer to LS1 and LS2 (*left*) and to DLS and SRA methods (*right*).

Results are presented in Figure 3 by subtracting the true motion from the calculated motion-correction parameters and show that both DLS and SRA methods are significantly robust to activation presence. The summary of correlation coefficients is presented in Table 1 (*right*).

param.	LS1	LS2	DLS	SRA	LS1	LS2	DLS	SRA
$t_x$	0.12	0.13	0.06	0.10	0.26	0.04	0.10	0.10
$t_y$	0.94	0.93	0.19	0.30	0.94	0.94	0.13	0.00
$t_z$	0.93	0.76	0.25	0.11	0.92	0.68	0.50	0.07
$r_x$	0.92	0.91	0.14	0.16	0.91	0.94	0.21	0.30
$r_y$	0.26	0.04	0.16	0.18	0.43	0.01	0.37	0.23
$r_z$	0.33	0.48	0.17	0.28	0.23	0.24	0.30	0.22

**Table 1.** Correlation values for the motionless simulated time series (*left*), and for the simulated time series with true activation-correlated motion (*right*).

### 3.3 Experiments with the Real Time Series

The four registration methods were also applied to three actual time series. For these datasets, the activation profile used to compute cross-correlation was obtained by convolving the task timing with the SPM99 hemodynamic model. A moving average was removed from the estimated motion parameters before computing the correlation in order to discard slow motion trends. In the case of the DLS method, the number of activated voxels in the three mask comprised, respectively, 19%, 22% and 18% of the brain size.

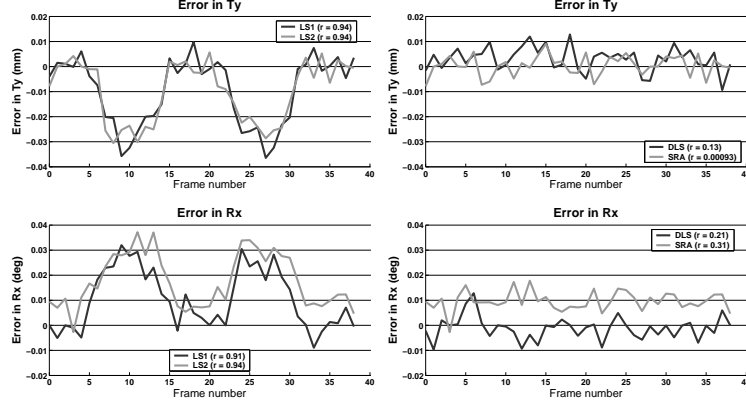


**Fig. 3.** Registration errors for the parameters  $t_y$  and  $r_x$  for the simulated time series with true correlated motion (true motion was removed). Graphs refer to LS1 and LS2 (left) and to DLS and SRA methods (right).

The results obtained with the three actual time series also indicate a reduction in the correlation between the motion estimates and the activation paradigm for the DLS and SRA. This is particularly visible in the  $t_y$  (and  $r_x$ ) parameter (see Figure 4). Correlation values are presented in Table 2.

For the first actual time series, one can see that the different methods do not generally agree in the estimation of  $r_y$  (and  $r_z$ ) parameter (see Figure 4). This effect, which is also observed for the other two time series, may be due to the fact that the methods do not share the same computational framework, as mentioned above.

param.	LS1	LS2	DLS	SRA	LS1	LS2	DLS	SRA	LS1	LS2	DLS	SRA
$t_x$	0.27	0.24	0.27	0.05	0.17	0.25	0.24	0.11	0.36	0.38	0.40	0.08
$t_y$	0.65	0.49	0.17	0.05	0.57	0.51	0.27	0.16	0.67	0.47	0.29	0.05
$t_z$	0.46	0.14	0.14	0.31	0.63	0.32	0.29	0.15	0.64	0.42	0.11	0.01
$r_x$	0.72	0.72	0.10	0.09	0.72	0.73	0.37	0.17	0.69	0.69	0.05	0.00
$r_y$	0.02	0.03	0.05	0.12	0.05	0.13	0.16	0.22	0.01	0.34	0.04	0.07
$r_z$	0.01	0.12	0.13	0.03	0.20	0.40	0.03	0.09	0.38	0.31	0.17	0.03

**Table 2.** Correlation values for the three real time-series.

## 4 Discussion

The problem of minimizing the bias introduced by the presence of activation is of particular importance due to the use of high field magnets ( $> 3T$ ), which increase

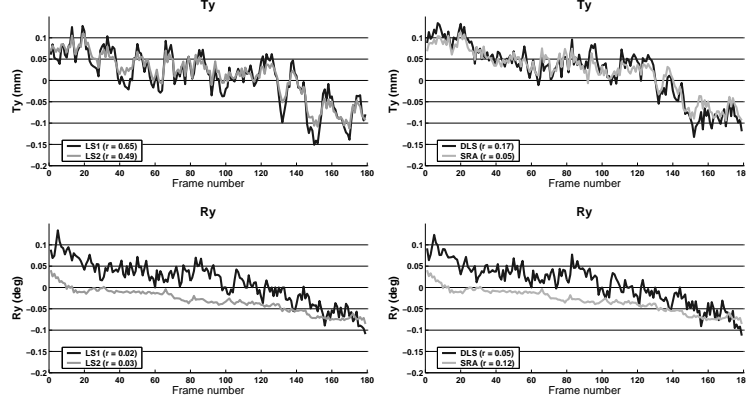


**Fig. 4.** Detrended registration parameters  $t_y$  and  $r_y$  for the first actual time series. Graphs refer to LS1 and LS2 (*left*) and to DLS and SRA methods (*right*).

activation amplitude. The work presented in this paper shows that the SRA and DLS methods seem suitable for the problem of motion compensation of FMRI studies, even in a situation where true activation-correlated subject motion is present. Indeed, this is an important issue when assessing the robustness of a registration method. The explanation is twofold: the first deals with the fact that interpolation errors during registration could be confounded with an activation-like bias; the second, to the well known fact that registration error (generally) increases with the initial misalignment.

The three actual time series used in this work were selected from among 14 subjects because they clearly presented a strong correlation with activation paradigm. Nevertheless, the true motion for these subjects is unknown and may or may not be correlated to the stimulus. However, the results obtained from the experiments performed in this paper clearly support the idea that the bias in motion estimates was due, at least in part, to presence of activation. Indeed, incorporating the activation profile into the SRA method or discarding about 20% of the voxels in the DLS method substantially reduces the correlation with the task.

A few plots obtained from the actual data show a disagreement between the different registration methods. In our opinion, this situation may stem from the fact that the time series include spatial distortions induced by the fast acquisition scheme. Indeed, there is an interaction between these distortions and head movement and therefore, the rigid registration approach cannot perfectly align the time series. In such ill-posed situations, similarity measures are prone to several local minima, which are due to local good matches between object features, possibly caused by the fact that both methods rely on different interpolation methods. This may explain why the two different computational frameworks

sometimes provide slightly different solutions for the rotation parameters for LS1 and LS2.

The success of the SRA method described in this paper calls for the development of integrated methods mixing motion estimation, activation detection and distortion correction. Like activation detection, however, distortion correction may require additional information, such as a magnetic field phase map obtained from the MR scan [9], adding another level of complexity because this phase map may depend on the head position in the scanner.

## 5 Conclusion

During the last decade, numerous general purpose similarity measures have been proposed to tackle medical image registration problems. They have led to a lot of success with important impact on neuroscience and clinical applications. The assumptions underlying these similarity measures, however, often neglect some features specific to fMRI data, leading to the kind of bias mentioned in this paper. In our opinion, tuning registration methods to account for these features, as demonstrated for the DLS and SRA methods, will be a necessary and fruitful endeavour.

## References

1. L. Freire and J.-F. Mangin, "Motion correction algorithms may create spurious brain activations in the absence of subject motion," *NeuroImage*, vol. 14 Sep, pp. 709–722, 2001.
2. M. Black and A. Rangarajan, "On the unification of line processes, outlier rejection, and robust statistics with applications in early vision," *International Journal of Computer Vision*, vol. 19, pp. 57–91, 1996.
3. C. Nikou, F. Heitz, J.-P. Armspach, I.-J. Namer, and D. Grucker, "Registration of MR/MR and MR/SPECT brain images by fast stochastic optimization of robust voxel similarity measures," *NeuroImage*, vol. 8(1) Jul, pp. 30–43, 1998.
4. L. Freire, A. Roche, and J.-F. Mangin, "What is the best similarity measure for motion correction of fmri time series?" *IEEE Trans. on Medical Imaging*, vol. 21(5) May, pp. 470–484, 2002.
5. L. Freire and J.-F. Mangin, "Two stage alignment of fmri time series using the experiment profile to discard activation related bias," in *Medical Image Computing and Computer-Assisted Intervention*, 2002, pp. 663–670.
6. J. Orchard, C. Greif, G. Golub, B. Bjornson, and M. Atkins, "Simultaneous registration and activation detection for fMRI," *IEEE Trans. on Medical Imaging*, vol. 22(11) Nov, pp. 1427–1435, 2003.
7. M. Unser, A. Aldroubi, and M. Eden, "B-spline signal processing: Part I-theory," *IEEE Trans Signal Process*, vol. 41, pp. 821–833, 1993.
8. W. Press, S. Teukolsky, W. Vetterling, and B. Flannery, *Numerical Recipes in C*, 2nd ed. Cambridge University Press, 1995.
9. C. Studholme, R. Constable, and J. Duncan, "Accurate alignment of functional EPI data to anatomical MRI using a physics-based distortion model," *IEEE Trans. on Medical Imaging*, vol. 19(11) Nov, pp. 1115–1127, 2000.